Provided for non-commercial research and education use.
Not for reproduction, distribution or commercial use.

This article was published in an Elsevier journal. The attached copy is furnished to the author for non-commercial research and education use, including for instruction at the author's institution, sharing with colleagues and providing to institution administration.

Other uses, including reproduction and distribution, or selling or licensing copies, or posting to personal, institutional or third party websites are prohibited.

In most cases authors are permitted to post their version of the article (e.g. in Word or Tex form) to their personal website or institutional repository. Authors requiring further information regarding Elsevier's archiving and manuscript policies are encouraged to visit:

http://www.elsevier.com/copyright

Author's personal copy

ELSEVIER

Available online at www.sciencedirect.com

ScienceDirect

Mechanics Research Communications 35 (2008) 50–56

MECHANICS
RESEARCH COMMUNICATIONS

www.elsevier.com/locate/mechrescom

Stress evolution to steady state in ion bombardment of silicon

Nagarajan Kalyanasundaram, Molly Wood [1], Jonathan B. Freund [2], H.T. Johnson *

Department of Mechanical Science and Engineering, University of Illinois at Urbana-Champaign, Urbana, IL 61801, United States

Received 14 August 2007
Available online 5 September 2007

Abstract

Low temperature ion bombardment of initially crystalline, defect-free silicon with 700 eV ion beam energy creates a highly-damaged stressed layer a few nanometers thick on the surface. An apparent steady state in structure is achieved at a fluence of 2×10^{14}–3×10^{14} ions/cm^2. In this work, the stresses are computed using the interatomic force definition of stress. The stress evolution is studied as a function of argon implantation into the target. Stress per implanted argon atom is observed to reach a nearly constant value between 20 MPa and 25 MPa at a fluence of 1.2×10^{14} ions/cm^2.
© 2007 Published by Elsevier Ltd.

Keywords: Stress evolution; Ion bombardment; Atomistic stress

1. Introduction

Ion bombardment of semiconductors like silicon and germanium using inert gas ion beams of argon, xenon or krypton is known to create regular, highly periodic, nanometer length scale surface patterns at ion fluences greater than 10^{16} ions/cm^2 (Ziberi et al., 2005; Gago et al., 2002; Ichim and Aziz, 2005). In these experiments, bombardment at medium ion beam energies (in the 0.5 keV to few keV ranges) of an initially defect-free and stress-free silicon target leads to a highly-damaged (amorphous) layer in the few nanometers near the surface (Moore et al., 2004; Haddeman and Thijsse, 2003). Effects of bombardment like sputtering of target atoms and stress creation in the target change as the target evolves to the highly-damaged state. Molecular dynamics (MD) simulations of silicon target bombarded with argons at 700 eV beam energy show the evolution of the target structure to an apparent steady state at fluences as low as 2×10^{14}–3×10^{14} ions/cm^2. Similarly, sputter yield evolution has been shown to evolve to steady state at fluences of 1×10^{14} ions/cm^2 (Moore et al., 2004). In this paper, the creation of an apparent steady state stress is analyzed from MD simulations of

* Corresponding author. Fax: +1 2172445977.
E-mail addresses: klynsndr@uiuc.edu (N. Kalyanasundaram), mcwood1@charter.net (M. Wood), jbfreund@uiuc.edu (J.B. Freund), htj@uiuc.edu (H.T. Johnson).
[1] Presently with Ace Industries, Norcross, GA 30093.
[2] Also in Aerospace Engineering.

0093-6413/$ - see front matter © 2007 Published by Elsevier Ltd.
doi:10.1016/j.mechrescom.2007.08.009

Author's personal copy

ion impacts. Once the structure, sputter yield, implantation and stress reach a steady state, the response of the surface to any further ion bombardment is expected to be free from transients or any anisotropy due to the crystalline bulk structure. Studying the response of such a steady state surface can yield useful insights in to the atomic-scale mechanisms that lead to pattern formation.

Stress development in thin-films due to ion bombardment and ion-assisted deposition has been the subject of many experiments and numerical simulations. An atomic peening model presented by d'Heurle (1970), d'Heurle and Harper (1989) demonstrates creation of a compressive stress in the target due to impinging ions. A model based on linear cascade sputtering theory and the atomic peening model predicts a linear dependence of compressive stress with ion flux and the square root of the energy (Windischmann, 1987). The stress in this model is given by

$$\sigma = K_1 f E_{\mathrm{B}}^{\frac{1}{2}} \delta \frac{EM}{(1-v)DN_0}, \tag{1}$$

where σ is the stress created in the target due to bombardment, K_1 is a proportionality factor, f is the ion flux, E_{B} is the ion beam energy, E is the elastic constant, v is the Poisson's ratio, D is the density of the target, M is the mass of the target and N_0 is the Avagadro number. δ contains information about the atomic numbers of the ion and target and is given by

$$\delta = \frac{Z_1 Z_2}{U_0}\left(1+\frac{M_1}{M_2}\right)^{\frac{1}{2}}\left(Z_1^{\frac{2}{3}}+Z_2^{\frac{2}{3}}\right)^{\frac{3}{4}}, \tag{2}$$

where Z_1 and M_1 are the atomic number and the mass of the ion, respectively, Z_2 and M_2 are the atomic number and the mass of the target atoms, respectively. U_0 is the surface binding energy. The dependence of the atomic numbers and the binding energies are contained in the term δ. The dependence of stress on ion and target masses, atomic numbers, working gas pressures, substrate orientation have all been studied (Windischmann, 1992). Eqs. (1) and (2) do not predict the evolution of the stress-free initially crystalline target in to a stressed, ion-bombarded target. It is assumed in these models that the material properties like the elastic constants do not change during bombardment as the material evolves from a crystalline state to a highly-damaged state.

Experimentally, ion bombardment with keV ion beam energies is shown to result in a compressive stress in the material (Chan et al., 2007). Ion bombardment in the MeV energy range on silicon wafers leads to an increasing compressive stress, followed by a decrease and then saturation in the compressive stress with increasing fluence (Volkert, 1991). Transitions between tensile and compressive stress regimes with increasing fluences have been observed in materials other than silicon (van Dillen et al., 1999; Lee et al., 1999; Zhang et al., 2003). van Dillen et al. (1999) propose a viscous flow relaxation model to explain stress evolution due to ion bombardment. Stress evolution has also been studied in atomistic simulations by Zhang et al. (2003) and Mayr and Averback (2005). In the work by Zhang et al. molecular dynamics simulations of stress evolution have been performed on self-bombarded carbon targets in the 1–150 eV beam energy range (Zhang et al., 2003). A steady state stress of 2–6 GPa has been calculated using the virial definition when the ion energies are between 30 eV and 150 eV after low fluences for carbon targets.

In this work, we first present the different formulations that are available to compute stresses in an atomistic system. Then, the suitability of these formulations to compute stress in ion-damaged targets is discussed. In the subsequent sections, results from MD simulations of stress evolution due to argon impacts on silicon and implantation evolution are presented until a fluence at which there is an apparent steady state in the stress induced by bombardment.

2. Atomistic stress definitions

In an atomistic simulation, such as a classical molecular dynamics simulation or a Monte Carlo simulation, the atomic positions and velocities are solved by integrating the equations of motion. In order to link the atomic positions and momenta to a macroscopic (continuum) stress, many different formulations like the virial

Author's personal copy

stress, the Hardy stress (Hardy, 1982), the BDT stress (Basinski et al., 1971), the Lutsko stress (Lutsko, 1988) and the interplanar mechanical stress exist.

The virial definition of stress is derived from a generalization of the virial theorem presented by Clausius (1870), Irving and Kirkwood (1950). The virial definition of stress component σ_{11} for a system modeled using two-body and three-body interactions is given by

$$\sigma_{11} = \frac{1}{\Omega}\left(\sum_i m_i v_i^2 + \sum_i \sum_{j>i} x_{ij} f_2^x(\mathbf{r}_i, \mathbf{r}_j)\right) + \frac{2}{\Omega}\left(\sum_i \sum_{j>i} \sum_{k>j} [x_{ij} f_3^x(\mathbf{r}_i, \mathbf{r}_j, \mathbf{r}_k) + x_{kj} f_3^x(\mathbf{r}_k, \mathbf{r}_i, \mathbf{r}_j)]\right), \tag{3}$$

where Ω refers to the system volume, m^i is the mass of atom i, $\mathbf{v}^i$ is the velocity of particle i, x_{ij} is the x_1 component of the position vector $\mathbf{r}_{ij} = \mathbf{r}_i - \mathbf{r}_j$, $f_2^x(\mathbf{r}_i, \mathbf{r}_j)$ refers to the component of two-body force between atoms i and j, and $f_3^x(\mathbf{r}_i, \mathbf{r}_j, \mathbf{r}_k)$ is the x_1 component of three-body interaction between atoms i, j, and k. The three-body terms, $f_3^x(\mathbf{r}_i, \mathbf{r}_j, \mathbf{r}_k)$, are zero for silicon–argon and argon–argon interactions. In deriving the virial formula, it is assumed that the material undergoes a homogeneous deformation. The unsuitability of the virial stress definition to the ion-bombarded target stems from the homogeneous target assumption. Cheung and Yip (1991) show that the virial definition cannot be interpreted meaningfully in the presence of inhomogeneities like free surfaces. An example of the highly-damaged target in which stresses are computed in the near-surface region is shown in Fig. 1. In fact, using the virial definition of stress for an ion-damaged target gives results that are contrary to experimental observations. Using virial stress definition for computing stress in the target bombarded with 500 eV ions, a tensile stress of 13 GPa is observed after a fluence of 2.64×10^{14} ions/cm^2. However, micromirror curvature correction experiments in which thin-film silicon MEMS micromirrors are bombarded with argons at similar energies show a compressive stress in the target. Furthermore, at the energy ranges considered in this work, many (>75%) of the incident argon atoms are implanted into the target, increasing target density. The implantation and densification of the target will give rise to a compressive stress; however, this contradicts the results from the virial stress calculations (Kalyanasundaram et al., 2005).

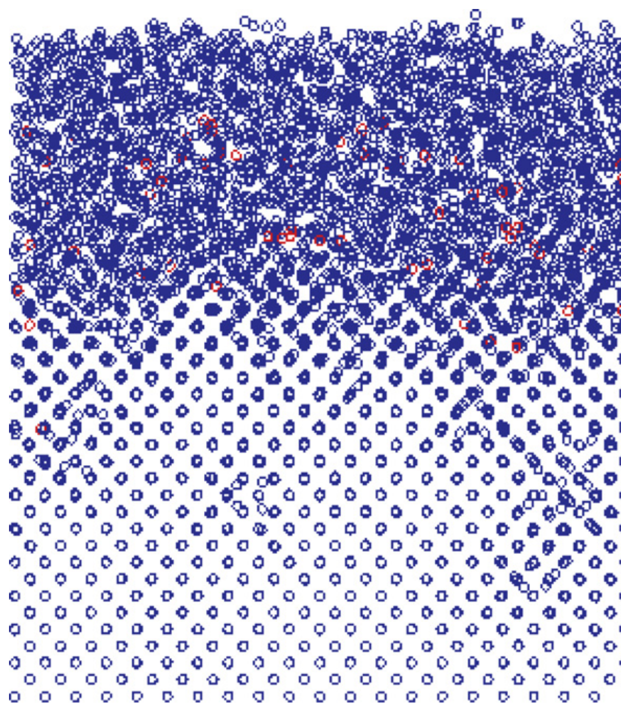

Fig. 1. Silicon target ion-bombarded with argon atoms up to a fluence of 2.61×10^{14} ions/cm^2. The view is a projection along the [010] direction, with a domain size of 5.43 nm × 5.43 nm. A highly-damaged layer is created near the surface and a nearly crystalline bulk layer is observed beneath the damaged layer. Blue denotes silicon and red denotes argon. (For interpretation of the references in colour in this figure legend, the reader is referred to the web version of this article.)

Author's personal copy

Other stress definitions like the BDT stress or the Hardy stress also make assumptions similar to the assumptions made in deriving the virial stress. The BDT stress, by definition, calculates a bulk homogeneous stress tensor. The BDT atomic stress is given by

$$\sigma_{\mathrm{ij}} = \frac{1}{\Omega_\alpha}\left(\frac{1}{2}m^\alpha v_i^\alpha v_j^\alpha - \frac{1}{2}\sum_\beta \frac{\partial V}{\partial r^{\alpha\beta}}\frac{r_i^{\alpha\beta} r_j^{\alpha\beta}}{|\mathbf{r}^{\alpha\beta}|}\right), \tag{4}$$

where V is the interatomic potential energy function, m^α is the mass of the atom α, v_i^α is its velocity component in the x_ith direction, $\mathbf{r}^{\alpha\beta}$ denotes the position vector joining atom α from atom β and Ω^α is the small volume in which the stress is computed. This definition of stress cannot be used for an inhomogeneous deformation.

The Lutsko stress formulation and extensions to it by Cormier et al. (2001) are based on computing the local stress tensor using statistical mechanics. Once again, this definition can only be applied when the stress state is homogeneous. The Lutsko stress can be thought of as a modification of the BDT stress tensor and is given by

$$\hat{\sigma}_{ij} = \frac{p_i^\alpha p_j^\alpha}{m^\alpha}\exp[\mathbf{iq}\cdot\mathbf{r}] - \frac{1}{2}\sum_{\alpha\neq\beta}\frac{\partial V}{\partial r^{\alpha\beta}}\frac{r_i^{\alpha\beta} r_j^{\alpha\beta}}{|\mathbf{r}^{\alpha\beta}|}\left[\frac{1-\exp[-\mathbf{iq}\cdot\mathbf{r}^{\alpha\beta}]}{\mathbf{iq}\cdot\mathbf{r}^{\alpha\beta}}\right]\exp[\mathbf{iq}\cdot\mathbf{r}^\alpha], \tag{5}$$

where $\hat{\sigma}_{ij}$ is the Fourier transform of the stress tensor σ_{ij}, $\mathbf{q}$ is a wavevector in Fourier space. p_i^α is the canonical momentum along the x_i-direction of atom α, m^α represents the mass of atom α, $\mathbf{r}^\alpha$ is the position vector of atom α and $\mathbf{r}^{\alpha\beta}$ denotes the position vector joining atom α from atom β. The definition can be inverted and written in a form similar to the BDT definition as

$$\sigma_{ij} = \frac{1}{\Omega_{\mathrm{average}}}\left(\frac{1}{2}m^\alpha v_i^\alpha v_j^\alpha - \frac{1}{2}\sum_\beta \frac{\partial V}{\partial r^{\alpha\beta}}\frac{r_i^{\alpha\beta} r_j^{\alpha\beta}}{|\mathbf{r}^{\alpha\beta}|}\right), \tag{6}$$

where $\Omega_{\mathrm{average}}$ is a small average volume in which the stress state is assumed to be homogeneous (Chandra et al., 2004). Cormier et al. show that the Lutsko stress can be calculated for an inhomogeneous deformation problem as long as the stress state is homogeneous within $\Omega_{\mathrm{average}}$. The Fourier transform approach assumes that the system has infinite spatial extent. A rigorous definition is not available when discontinuities like surfaces and interfaces are present (Zimmermann et al., 2004). Due to the presence of surfaces and a boundary between damaged and mostly-crystalline regions in the ion-bombarded target, the Lustko stress definition is not applicable to ion-bombarded targets.

The Hardy stress definition is similar to Lutsko's stress definition and is given in Zimmermann et al. (2004). Stress calculated using the Hardy formalism has also been demonstrated to fluctuate near the surface, though the fluctuations are considerably smaller than those in the virial formalism (Zimmermann et al., 2004). The Hardy definition is, therefore, not suitable for ion-bombarded targets. Instead, the interplanar mechanical stress method, as described in Kalyanasundaram et al. (2005), is used here to calculate stresses in ion-bombarded silicon. The method, as applied to the ion-bombarded target, is discussed in the next section along with the results of stress evolution.

3. Stress evolution due to ion bombardment

Cheung and Yip presented the interatomic force-balance definition of stress in Cheung and Yip (1991). In defining this stress, a cross-section of area A is considered in the target. The σ_{11} component using the interatomic force-balance definition is given by

$$\sigma_{11} = \frac{1}{A}\left[\frac{1}{2}\sum_i \frac{m^i v_1^i}{\Delta t} + \sum_i\sum_{j>i}\mathbf{F}_{ji}(\mathbf{r}_{ij})\cdot\mathbf{e}_1\right], \tag{7}$$

where $\mathbf{F}_{ji}$ is the two-body force vector on atom j due to i, $\mathbf{e}_1$ is the unit vector along the x_1 axis, $\mathbf{r}_{ij}$ is the position vector of a point in the plane where stress is computed, m_i and v_1^i are the mass of the ith atom and component of velocity of the ith atom along x_1 direction, respectively.

Author's personal copy

At low target temperatures, when the configuration of the target is nearly static and the kinetic energy or the momenta are negligible, the stress computed using the interatomic force-balance definition at some cross-section in the target is the force-field acting on a plane per unit area. For a target that is modeled by two-body and three-body forces, the traction can be written as

$$\mathbf{t}_n = \frac{1}{A}\left(\sum_i \sum_{j>i} \mathbf{F}_{ji}(\mathbf{r}_{ij}) + \sum_i \sum_{j>i} \sum_{k>j} \mathbf{F}_{jki}(\mathbf{r}_{ij}, \mathbf{r}_{kj}, \theta_{ijk})\right), \tag{8}$$

with

$$\mathbf{n}_i \cdot \mathbf{n}_j < 0, \tag{9}$$

$$\mathbf{n}_i \cdot \mathbf{n}_k < 0, \tag{10}$$

and

$$\sigma_{11} = \mathbf{t}_n \cdot \mathbf{e}_1, \tag{11}$$

where A is cross-sectional area, $\mathbf{F}_{ji}$ is the force vector on atom j due to i, $\mathbf{F}_{jki}$ is the force on atom j due to atoms k and i, $\mathbf{n}_i$ is the unit vector passing through atom i normal to the plane, and $\mathbf{e}_1$ is the unit vector along the x_1 axis. Details of the MD simulations of ion impacts and the stress calculation procedure are presented in Moore et al. (2004), Kalyanasundaram et al. (2005). A thermostat used in the MD simulations maintains a bulk temperature of 77 K. The stresses are computed in the targets after freezing the defects to 4 K in order to obtain a static configuration. As shown in Kalyanasundaram et al. (2005), the calculations performed using the interatomic force-balance definition agree well with the tensile/compressive character of stress and also with the magnitude of the stress.

Using the interatomic force-balance definition, atomistic studies of stress evolution in silicon in the medium energy regimes show three regimes of stress evolution. The first regime, where the stress is tensile, has been explained to be due to the initial damage to the defect-free surface and occurs before the structure has evolved into a highly-damaged target.

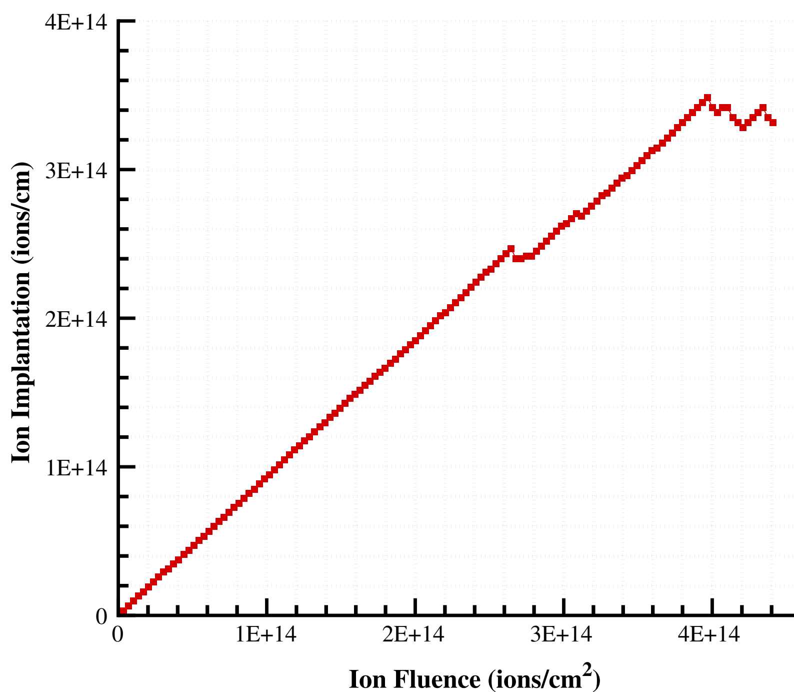

Fig. 2. Evolution of implantation of argon atoms into the target bombarded at 700 eV. Initially, >75% of incident argons are implanted into the target. After a fluence of about 3.5×10^{14} ions/cm^2, the number of implanted atoms in the target reaches a steady state.

Author's personal copy

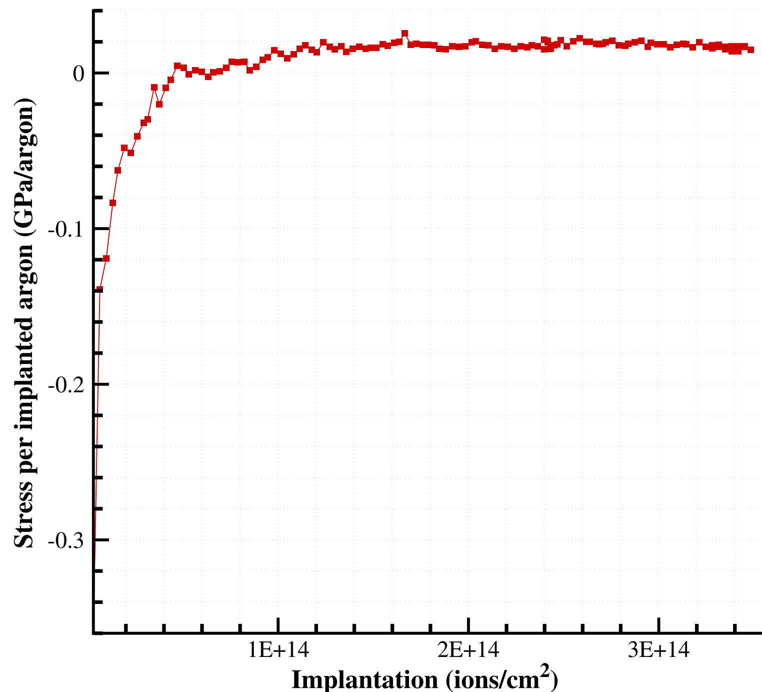

Fig. 3. Dependence of stress on number of implanted atoms. Compressive stress (positive) per implanted argon is nearly constant after a fluence of 7×10^{13} ions/cm^2. Since the number of implanted argons reach a steady state after ion fluence of 3.5×10^{14} ions/cm^2, stress also reaches a steady state.

The evolution of stress in the second and the third stage of evolution are explained to be due to implantation of argons into the target (Kalyanasundaram et al., 2005). First, the evolution of implantation is plotted in Fig. 2 as a function of incident ion fluence. The implantation of argons into the initially defect-free crystalline target increases linearly at low fluences. However, after a fluence of 3.5×10^{14} ions/cm^2, the implantation behavior changes from an increasing trend into an oscillation about a steady value.

Fig. 3 shows the evolution of stress per implanted argon as a function of the implanted argons. The stresses are computed using the interatomic mechanical stress definition on a 5.43 nm × 5.43 nm cross-section defined in the target. Compressive stress is set in the target at a low initial fluence of about 7×10^{13} ions/cm^2. At typical experimental fluxes of $10^{13} - 10^{15}$ ions/cm^2 s, this onset of compressive stress occurs in less than a few seconds of ion bombardment. The stress per implanted ion then reaches a steady state at an ion fluence of approximately 1.5×10^{14} ions/cm^2. As the ion fluence increases to 3.5×10^{14} ions/cm^2, the implantation behavior changes to oscillate about a steady value. The compressive stress calculated in the 5.43 nm × 5.43 nm cross-section continues to increase to about 1.62 GPa (8.8 N/m) and saturates at this value at a fluence above 3.5×10^{14} ions/cm^2.

The stress evolution shown in Fig. 3 can be explained using a point-defect model. In the point-defect model, an argon atom is assumed to be implanted as a point-defect in a crystalline silicon target at an interstitial site. The traction for such a point-defect model is calculated to be 30.0 MPa per implanted argon. This point-defect model is expected to overpredict the stress rate because, in this model no structural relaxation is assumed in the target after implantation. No viscous relaxation mechanism is modeled in this work and it appears that the stress can be modeled as a function of implantation. The stress per implanted argon value agrees reasonably well with the values computed from the MD simulations (about 20–25 MPa per implanted argon).

4. Conclusions

Various definitions of stress that connect the atomic positions and velocities to macroscopic stress were presented. Stress evolution in a nanometer length scale silicon target due to argon bombardment at 700 eV is studied using an interatomic mechanical stress method. The applicability of other definitions like the virial

Author's personal copy

stress was discussed. A saturation in the number of implanted argons is observed after a fluence of 3.5×10^{14} ions/cm^2. Stress per implanted argon is nearly constant, the magnitude of which can be explained using a point-force model. Due to the saturation in the number of implanted argons, stress due to bombardment saturates at fluences as low as 3.5×10^{14} ions/cm^2. At typical experimental fluxes, this fluence corresponds to a few seconds of ion bombardment. The saturation stress is 1.62 GPa (8.80 N/m) for the 700 eV case.

Acknowledgements

Support for this work came from NSF (CMS05-10624) and the Computational Science and Engineering program at the University of Illinois at Urbana-Champaign. The molecular dynamics simulations were run on University of Illinois' Turing Xserve Cluster.

References

Basinski, Z.S., Duesberry, M.S., Taylor, R., 1971. Canadian Journal of Physics 49, 2160.
Chandra, N., Namilae, S., Shet, C., 2004. Physical Review B 69, 094101.
Chan, W.L., Chason, E., Iamsumang, C., 2007. Nuclear Instruments and Methods in Physics Research Section B – Beam Interactions with Materials and Atoms 257, 428.
Cheung, K.S., Yip, S., 1991. Journal of Applied Physics 70, 5688.
Clausius, R., 1870. Philosophical Magazine 40, 122.
Cormier, J., Rickman, J.M., Delph, T.J., 2001. Journal of Applied Physics 89, 99.
d'Heurle, F.M., 1970. Metallurgical Transactions 1, 725.
d'Heurle, F.M., Harper, J.M.E., 1989. Thin Solid Films 171, 81.
Gago, R., Vazquez, L., Cuerno, R., Varela, M., Ballesteros, C., Albella, J.M., 2002. Nanotechnology 13, 304.
Haddeman, E.F.C., Thijsse, B.J., 2003. Nuclear Instruments and Methods in Physics Research Section B – Beam Interactions with Materials and Atoms 202, 161.
Hardy, R.J., 1982. Journal of Chemical Physics 76, 622.
Ichim, S., Aziz, M.J., 2005. Journal of Vacuum Science Technology B 23, 1068.
Irving, J., Kirkwood, J.G., 1950. Journal of Chemical Physics 18, 817.
Kalyanasundaram, N., Freund, J.B., Johnson, H.T., 2005. Journal of Engineering Materials and Technology 127, 457.
Lee, D.H., Fayeulle, S., Walter, K.C., Nastasi, M., 1999. Nuclear Instruments and Methods in Physics Research Section B – Beam Interactions with Materials and Atoms 148, 216.
Lutsko, J.F., 1988. Journal of Applied Physics 64, 1152.
Mayr, S.G., Averback, R.S., 2005. Physical Review B 71, 134102.
Moore, M.C., Kalyanasundaram, N., Freund, J.B., Johnson, H.T., 2004. Nuclear Instruments and Methods in Physics Research Section B – Beam Interactions with Materials and Atoms 225, 241.
van Dillen, T., Brongersma, M.L., Snoeks, E., Polman, A., 1999. Nuclear Instruments and Methods in Physics Research Section B – Beam Interactions with Materials and Atoms 148, 221.
Volkert, C., 1991. Journal of Applied Physics 70, 3521.
Windischmann, H.J., 1987. Journal of Applied Physics 62, 1800.
Windischmann, H.J., 1992. Critical Review of Solid State Materials Science 17, 547.
Zhang, S., Johnson, H.T., Wagner, G.T., Liu, W.K., Hsia, K.J., 2003. Acta Materialia 51, 5211.
Ziberi, B., Frost, F., Höche, T., Rauschenbach, B., 2005. Physical Review B 72, 235310.
Zimmermann, J.A., Webb, E.B., Hoyt, J.J., Jones, R.E., Klein, P.A., Bammann, D.J., 2004. Modelling and Simulation in Materials Science and Engineering 12, S319.